






Cite this: *Chem. Sci.*, 2023, 14, 2379

All publication charges for this article have been paid for by the Royal Society of Chemistry

Transition metal-free photochemical C–F activation for the preparation of difluorinated-oxindole derivatives†

Bianca Matsuo, ^{‡a} Jadab Majhi, ^{‡a} Albert Granados, ^a Mohammed Sharique,^a Robert T. Martin, ^b Osvaldo Gutierrez^{*bc} and Gary A. Molander ^{*a}

The development of strategies for single and selective C–F bond activation represents an important avenue to overcome limitations in the synthesis of valuable fluorine-containing compounds. The synthetic and medicinal research communities would benefit from new routes that access such relevant molecules in a simple manner. Herein we disclose a straightforward and mechanistically distinct pathway to generate *gem*-difluoromethyl radicals and their installation onto *N*-arylmethacrylamides for the preparation of valuable difluorinated oxindole derivatives. To achieve operational simplicity, the use of a readily available benzenethiol as a photocatalyst under open-to-air conditions was developed, demonstrating the facile multigram preparation of the targeted fluorinated molecules. Additionally, dispersion-corrected density functional theory (DFT) and empirical investigations provide a new basis to support the proposed reaction pathway, indicating that arene thiolate is an efficient organophotocatalyst for this transformation.

Received 9th November 2022

Accepted 2nd February 2023

DOI: 10.1039/d2sc06179a

rsc.li/chemical-science

Introduction

Challenging synthetic organic transformations have driven the development of new protocols to diversify and broaden existing methods. New technologies and activation modes have dramatically changed how chemical space is being explored. Among the various challenges in the field, the selective activation of a single C–F bond in polyfluorinated substrates has become a desirable transformation.^{1–3} The inherent interest in accessing C–F bond-containing molecules is attributed to the fact that these bonds are prevalent in biologically active compounds. Fluorinated molecules have proved to be key in drug discovery programs because they can dramatically change the properties of drug candidates by improving stability, permeability, and, consequently, the efficacy of molecules discovered therein.^{4,5} It is not a coincidence that fluorinated molecules are highly represented in many currently marketed drugs. Consequently, continuous efforts have been made to prepare and derivatize such molecules. A central challenge in this synthetic field remains the high bond dissociation energy

of C–F bonds, which imposes limitations on selective bond cleavage and further functionalization in polyfluorinated substrates.

Considering modern approaches to this challenge, electrochemical and photochemical methods have emerged as extremely useful technologies, allowing selective C–F bond activation in various different classes of compounds,^{3,6} including fluoroarenes,^{7–13} trifluoromethylated arenes^{14–17} and -alkenes,^{18–23} *gem*-difluoroalkenes,^{24–29} and others, such as trifluoromethylated esters, -amides,^{30–33} and -ketones³⁴ under mild reaction conditions.

In this arena, photoinduced metal-free protocols represent a highly attractive approach to C–F activation, providing valuable structures without trace metals; a feature that is especially relevant in the industrial sector. Small organic conjugated molecules have been shown to exhibit interesting properties as photocatalytic species, successfully allowing C–F bond activation. Some examples include the use of pyrenes³⁵ and phenoxazines¹⁵ in catalytic hydrodefluorination of polyfluoroarenes and trifluoromethylarenes, respectively; the exploration of phosphinophenolates³² in defluoroalkylation and hydrodefluorination of trifluoromethylated substrates [*e.g.*, esters, acetamides, and (hetero)arenes]; in addition to the well-known applications of dicyanobenzenes as potent organophotocatalysts.^{16,33,36}

In 2021, our group disclosed a metal-free and mechanistically novel approach to install *gem*-difluoromethylene groups from trifluoroacetates and -acetamides onto (un)activated alkenes.³⁰ The method was designed to be promoted by a hydrogen atom transfer (HAT) step *via* combination of diaryl

^aRoy and Diana Vagelos Laboratories, Department of Chemistry, University of Pennsylvania, 231 South 34th Street, Philadelphia, Pennsylvania 19104-6323, USA. E-mail: gmolandr@sas.upenn.edu

^bDepartment of Chemistry and Biochemistry, University of Maryland, 8051 Regents Drive, College Park, Maryland 20742, USA

^cDepartment of Chemistry, Texas A&M University, 580 Ross St., College Station, Texas 77843, USA. E-mail: og.labs@tamu.edu

† Electronic supplementary information (ESI) available. See DOI: <https://doi.org/10.1039/d2sc06179a>

‡ B. M. and J. M. contributed equally.

ketone, thiol, and sodium formate. Continuing with our interest in the synthesis of fluorinated compounds *via* photoredox catalysis,^{19,21,22,37–39} we focused on developing a metal-free preparation of difluorinated oxindole derivatives *via* a cascade reaction between *gem*-difluoromethylene radicals and *N*-aryl-methacrylamides, exploring the photoreactive nature of thiols as photocatalysts.

Aryl acrylamides are useful precursors to build more complex structures containing the oxindole moiety, known to exhibit extraordinary activities as drugs as well as being present in many active natural products.^{40–42} They have been explored in cascade-type transformations where the sequence of addition to the alkene moiety followed by cyclization and rearomatization leads to interesting and valuable compounds from a medicinal point of view. Our approach would represent a complementary and alternative route to access these privileged motifs under milder conditions, extending the chemical space covered by previous advances in the field, which have demonstrated the use of trifluoromethylated arenes¹⁷ and -ketones³⁴ as *gem*-difluoromethylene radical sources. In these examples, activation of the C–F bond was achieved by employing a combination of Ir-catalysts and Lewis acids to facilitate the fluoride elimination (Fig. 1a).

Previous approaches to installing *gem*-difluoroacetates for the preparation of valuable difluorinated oxindoles make use of harsh conditions in the presence of metal-based catalysts, oxidants, and/or high temperatures, and are restricted regarding the structural diversification of the fluorinated moiety (Fig. 1b).^{43–46} Recently, a seminal Giese addition protocol using trifluoromethylated compounds was also reported by the Shang group, supporting the application of thiolate species as reductants and HAT catalysts. An efficient hydrodefluorination of trifluoroacetates, -arenes, and -amides and the coupling with a range of alkenes was reported (Fig. 1c).³¹ In another vein, Chiba and co-workers explored the powerful ability of photo-excited thiol anions to promote the single-electron reduction of aryl halides with reduction potentials as low as -2.4 V *vs.* SCE,^{47,48} while Hamashima explored thiobenzoic acid as a single-electron reducing agent and HAT agent to promote regioselective α -H arylation reactions.⁴⁹ All of these precedents demonstrate the rich applicability of sulfur anions as potential photocatalysts.⁵⁰

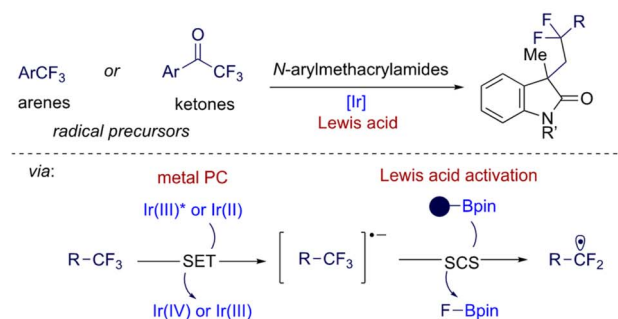
Seeking alternative methods that would provide easy access to *gem*-difluoromethyl radicals under metal-free and milder conditions, we recognized that benzenethiols play a key role as photocatalysts under blue and purple light irradiation and, in the presence of sodium formate,^{30–32,36,51,52} directly lead to selective mono C–F bond cleavage in trifluoroacetates. Herein, we report a transition metal-free, mild, and operationally simple method to overcome the limitations associated with the preparation of fluorinated oxindole molecules by single C–F bond activation (Fig. 1d).

Discussion

To initiate our studies, we chose 4-methoxybenzenethiol as a catalytic species. The screening of the reaction conditions for

a. C(sp³)-F bond cleavage in trifluoromethylated arenes and -ketones, merging photoredox catalysis and Lewis Acid activation

•König (2017), Qu and Chatterjee (2021)

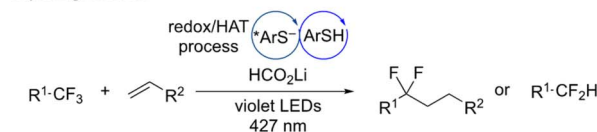


b. Other protocols for the installation of ethyl *gem*-difluoroacetate radicals onto *N*-arylmethacrylamides



•metal catalysts •high temperatures •lack of structural diversity

c. Defluoroalkylation and hydrodefluorination of trifluoromethyl compounds exploring thioliates



d. This work: photoinduced, metal-free approach

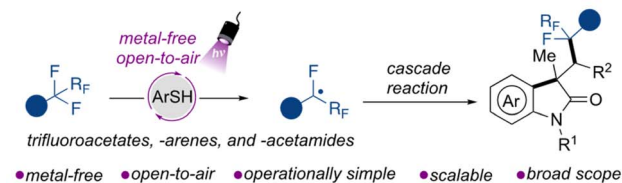
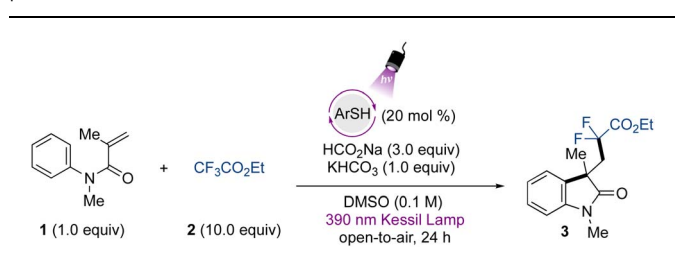


Fig. 1 Previous approaches to preparing difluoroalkylated compounds.

the defluorinative alkylation protocol between the *N*-arylmethacrylamide **1** and the trifluoroacetate **2** demonstrated that the use of 20 mol% of the organophotocatalyst, in combination with sodium formate and KHCO_3 , provides access to the corresponding difluorinated oxindole **3** in 95% yield under 390 nm wavelength LED irradiation (Table 1, entry 1). Lowering the catalyst loading led to erosion of the yield (Table 1, entry 2). The use of excess trifluoroacetate provided high yields, however the utilization of fewer equivalents also gave the product in moderate yields (Table 1, entry 3) (see Table S1 for the complete optimization, ESI†). Because this source of *gem*-difluoromethylene radical is a commercially available, bench-stable, and cost-accessible material in comparison to bromo/iodo-difluoroacetates, we decided to proceed with the use of 10 equivalents for the study of this transformation.

Notably, the reaction successfully takes place under an oxygen atmosphere, and no degassing of the reaction is required. These results indicate the operational simplicity of the developed protocol, and the open-to-air conditions still lead to excellent results even though oxygen is known to oxidize



Table 1 Optimization of the metal-free defluorinative alkylation protocol^a

| Entry | Deviation from std condition | Yield ^b (%) |
|----------------|------------------------------|------------------------|
| 1 | None | 95 |
| 2 | 0.10 equiv. of ArSH | 50 |
| 3 | 7.0 equiv. of 2 | 64 |
| 4 | No base | 56 |
| 5 | 1.0 equiv. of sodium formate | 10 |
| 6 | Violet Kessil 427 nm | 10 |
| 7 ^c | No Kessil lamp | nr |

^a Reaction conditions: **1** (0.1 mmol, 1 equiv.), **2** (10 equiv.), ArSH (0.20 equiv.), HCO₂Na (3.0 equiv.) and KHCO₃ (1.0 equiv.) in DMSO (0.1 M) under 390 nm wavelength Kessil light irradiation and open-to-air.

^b Yields determined by ¹⁹F NMR analysis using 4-bromo-2-fluoro-1-iodobenzene as internal standard. ^c Reaction performed under heating at 60 °C. ArSH = 4-methoxybenzenethiol.

thiols.⁵³ Preliminary studies were carried out in DMSO, and in the presence of other polar aprotic solvents, no product formation was observed. Other alternative sulfoxide and sulfone-based solvents, such as tetramethylene sulfoxide and sulfolane, did not lead to formation of the desired product (see ESI†). The use of base was also important to achieve high yields (Table 1, entry 4), and sodium formate was demonstrated to be a crucial component for the reaction to take place (Table 1, entry 5). Regarding the irradiation source, the photocatalyst showed poor activity under 427 nm wavelength Kessil irradiation (Table 1, entry 6). As control experiments, no transformation occurred in the absence of irradiation (Table 1, entry 7) or using TEMPO as a radical scavenger, indicating the radical nature of the transformation.

To demonstrate the applicability of the developed metal-free protocol, we prepared a library of oxindole derivatives containing diverse functional groups attached to the aromatic ring of the *N*-arylmethacrylamide component, as well as other diverse substructural motifs (Fig. 2). As expected, electron-donating groups were amenable to this photochemical difluoroalkylation protocol, providing compounds **4–6** with good yields. Halogen atoms were also successfully tolerated, with excellent compatibility with a *para*-fluoro substituent in **7**. Other halogen moieties such as chloride and bromide substituents in the *para*-, *meta*-, and *ortho* positions on the aromatic ring (**8–11**) also showed good reactivity. A naphthyl aromatic ring was also included, providing the corresponding difluorinated oxindole **12** with lower yield, which can be attributed to a competitive hydroarylation reaction leading to the formation of the benzodihydroquinolinone product.⁵⁴ The *gem*-difluoromethyl radical was also smoothly added to a 1,1-disubstituted olefin to provide compound **13** with

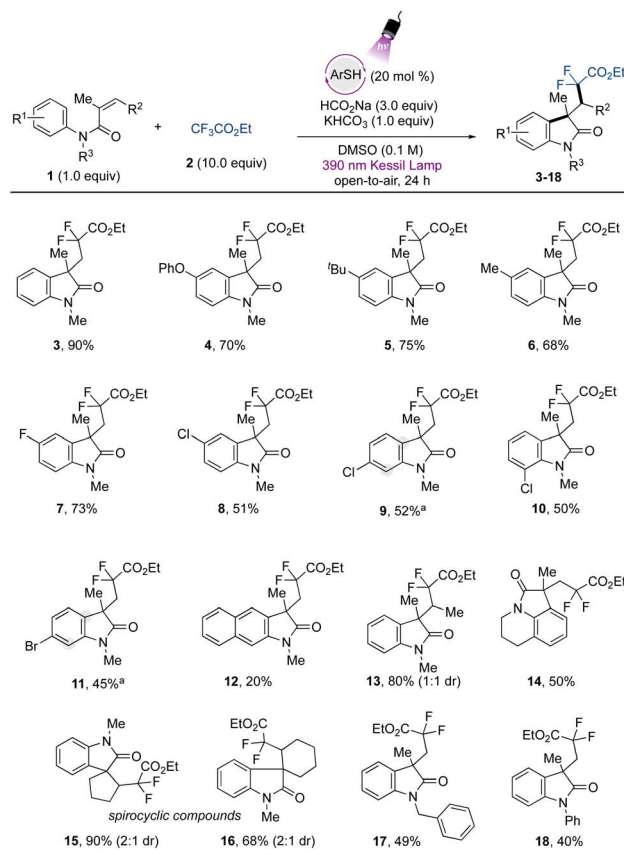


Fig. 2 Scope of *N*-aryl acrylamides in the cascade addition/cyclization reaction for the synthesis of difluorinated oxindoles. All values indicate the yield of the isolated product. Reaction conditions: *N*-arylmethacrylamide (0.5 mmol, 1 equiv.), **2** (10 equiv.), ArSH (0.20 equiv.), HCO₂Na (3.0 equiv.) and KHCO₃ (1.0 equiv.) in DMSO (0.1 M) under 390 nm wavelength Kessil light irradiation and open-to-air. ^a Obtained as a mixture of isomers. ArSH = 4-methoxybenzenethiol.

80% yield and 1 : 1 dr. Given the potential of the method, we further applied it to the preparation of more complex fused tricyclic compounds. The oxindole derivative derived from tetrahydroisoquinoline (**14**) was successfully obtained with moderate yield. Further examples to explore the scope included modification of the alkene moiety of the *N*-arylmethacrylamide. Spirocyclic compounds possess recognized relevance in biological chemistry and are considered challenging targets in organic synthesis.^{41,55} By using internal alkenes in five- and six-membered rings, spirocyclic compounds **15** and **16** were readily prepared in excellent yields. Finally, the benzyl- and phenyl protecting groups (**17** and **18**, respectively) were also tolerated under the developed protocol, while the unprotected or Boc-protected acrylamides or phenyl methacrylate precursors did not lead to the desired products.

Attention was next turned to verifying the fluoroalkylation of other trifluoromethylated compounds *via* the developed metal-free strategy. Extending the scope using trifluoroacetates, selective C–F bond cleavage was found to occur smoothly when other derivatives were employed (Fig. 3). For example, aliphatic ester-containing alkyl- and aromatic groups (as in phenethyl- (**19**) and 2-cyclohexylethyl- (**20**) trifluoroacetates) underwent the



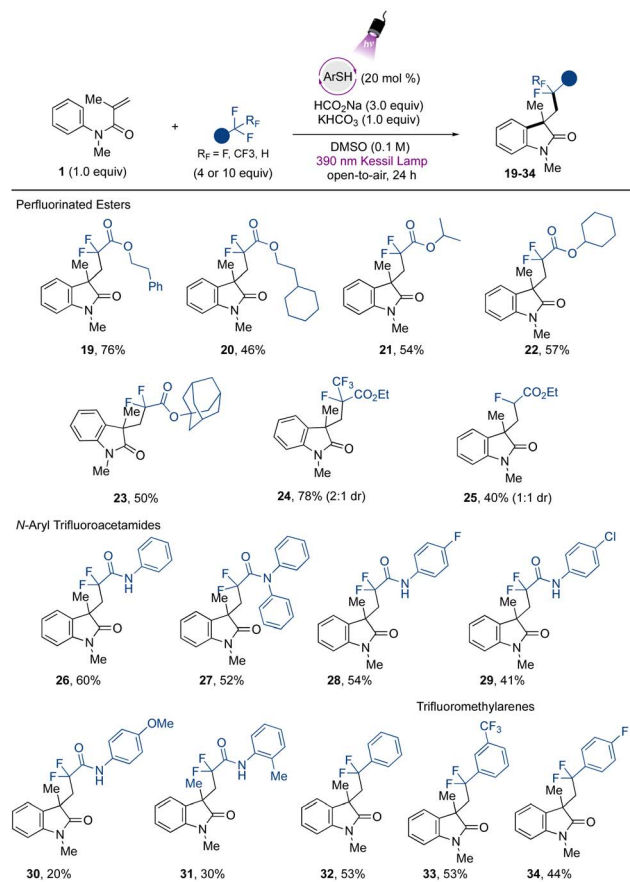


Fig. 3 Scope of trifluoromethylated compounds in the cascade addition/cyclization reaction for the synthesis of difluorinated oxindoles. All values indicate the yield of the isolated product. Reaction conditions: N -arylacrylamide **1** (0.5 mmol, 1 equiv.), trifluoromethylated compound (10 equiv. for the scope of trifluoroacetates and CF_3 -arenes, and 4 equiv. for the scope of acetamides), ArSH (0.20 equiv.), HCO_2Na (3.0 equiv.) and KHCO_3 (1.0 equiv.) in DMSO (0.1 M) under purple Kessil light irradiation and open-to-air. ArSH = 4-methoxybenzenethiol.

desired transformation with good to excellent yields. Other α,α -difluorinated aliphatic carboxylate esters containing secondary aliphatic groups were accessed, such as those in the isopropyl- (21), and cyclohexyl (22) derivatives, and the tertiary example containing the sterically demanding adamantyl group (23). Other challenging CF_3 -containing substrates were engaged in the cascade transformation. Ethyl pentafluoropropionate ($E_{\text{red}} = -2.6 \text{ V vs. SCE}$)³⁰ smoothly underwent regioselective single C–F bond activation to provide the corresponding difluoro-oxindole derivative **24** containing an intact CF_3 group in 78% yield. Additionally, **25**, derived from ethyl difluoroacetate, which presents an even more challenging reduction potential than other substrates ($E_{\text{red}} = -2.9 \text{ V vs. SCE}$),³⁰ was also successfully accessed, although in lower yield.

The protocol was further extended to trifluoromethylated amide precursors. Amide-containing compounds are valued structures from a medicinal and synthetic point of view, given the intrinsic properties associated with this functional group,

such as their polarity, stability, and H-bonding capability.⁵⁶ Difluorinated oxindole derivatives containing pendant amide-groups (**26–29**) were thus generated in modest to good yields. The trifluoroacetamide ($E_{\text{red}} = -2.2 \text{ V vs. SCE}$) gave direct access to the desired compound **26** from the defluorinative-cascade process in 60% yield, and the diphenyl derivative **27** was also accessed in modest yield. Interestingly from a synthetic point of view, the acetamides containing halogen atoms at the *para* position on the aromatic ring underwent the transformation in moderate to good yield (**28** and **29**). The thiolate excited-state presents a highly reducing power ($E_{\text{red}} = -3.3 \text{ V vs. SCE}$)³¹ capable of promoting a competitive homolytic C–X bond cleavage, which may be associated with the yields observed for halogenated compounds. Electron-rich acetamides provided poor results, as in **30** and **31**. Limitations were found regarding the use of acetamides containing electron-withdrawing groups, and the derivatives substituted with cyano- and di- CF_3 groups did not react under the developed conditions (see ESI for more information†). Although the method still presents opportunities to be explored to extend the scope regarding the use of structurally diverse amides, the method avoids the use of Lewis acids as additives, which are usually employed to lower the reduction potential of these species.³⁰ Finally, exploring the further potential of the developed method, the use of trifluoromethyltoluene provides access to the arylated difluoro-oxindole derivative **32** in 53% yield, and a similar yield was found when 1,3-(bis)trifluoromethyltoluene was evaluated (**33**). The scope also included the *p*-fluorotoluene derivative, which gave rise to **34** in 44% yield. For other halogenated arenes ($\text{X} = \text{Br}, \text{I}$), the homolytic C–X bond cleavage was observed instead, indicating the powerful reducing properties of the organophotocatalyst employed in the study. These results demonstrate the applicability of the method *via* another mechanistic approach, complementing the protocols disclosed recently introducing difluoromethyl ketones and -arenes under photocatalytic conditions.^{17,34}

Given the importance of the scalability of new synthetic methods aiming at industrial applications, we successfully achieved the preparation of 1.9 grams (10 mmol scale) of compound **3** in 64% yield under the standard reaction conditions. For this demonstration, we employed 4 equivalents of trifluoroacetate **2**, and the yield was comparable to the small-

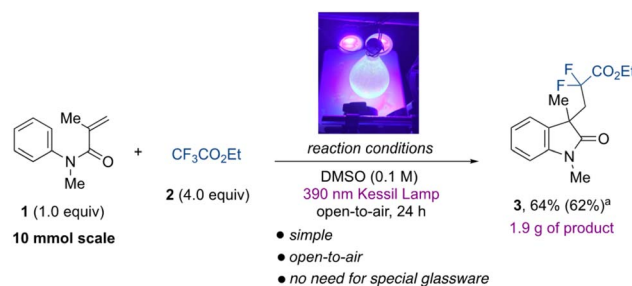


Fig. 4 Scalability of the defluorinative alkylation protocol for the large-scale preparation of difluorinated oxindoles. ^aYield for the 0.1 mmol scale reaction using 4.0 equiv. of **2**. ArSH = 4-methoxybenzenethiol.

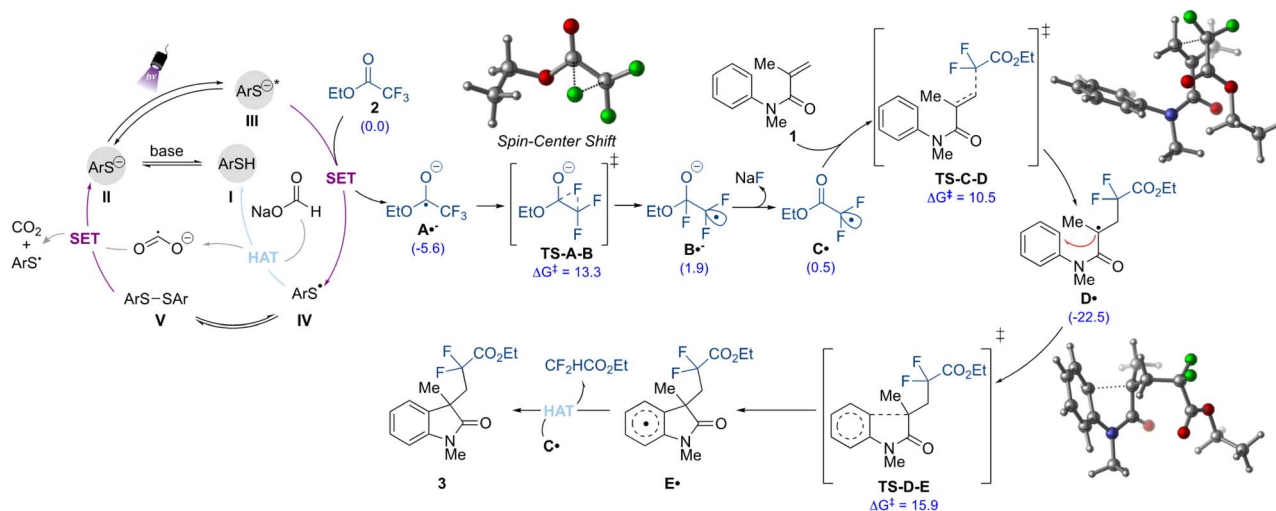


Fig. 5 Proposed mechanism for the metal-free defluorinative alkylation strategy. Free energies of relevant species reported in kcal mol⁻¹ at UωB97XD/def2-SVP-CPCM(DMSO)//UB3LYP-D3/def2-SVP-CPCM(DMSO) level of theory.

scale reaction (0.1 mmol). As noted in Fig. 4, the large-scale experiment was easily performed simply by using a large round-bottom flask irradiated with the 390 nm light source. The scope regarding the trifluoroacetates nicely complements and extends other reported protocols, allowing for the first time the installation of these motifs onto *N*-arylmethacrylamides *via* C–F bond activation.

Finally, to gain insights into the mechanism of this transformation, we employed dispersion-corrected density functional theory (DFT) computations (Fig. 5 and ESI†). As shown in Fig. 5, the proposed mechanism initiates with the formation of the thiolate species **II** from deprotonation of the thiol **I** in the presence of base. The thiolate **II** is then promoted to the excited anion (**III**) under purple light irradiation. Given the strong ability of the latter to act as a reductant ($E_{\text{red}} = -3.3$ V vs. SCE),³¹ the initial defluorinative step to form the radical anion species **A**^{•-} should take place *via* single electron reduction of the ethyl trifluoroacetate **2** ($E_{\text{red}} = -2.0$ V vs. SCE), as supported by quenching experiments.³⁰ In the thiolate catalytic cycle, the thiyl radical **IV** formed is prone to undergo dimerization, and it is in equilibrium with the disulfide **V**.

This species also demonstrated the ability to play a role as the pre-catalyst, providing product **3** with a 95% yield when used instead of **I** (Table S2, ESI†). Regeneration of the pre-catalyst **I** can then take place *via* HAT between **IV** and sodium formate. In this step, the reductant $\text{CO}_2^{\cdot-}$ is formed, which can also contribute to the generation of the active thiolate species **II** by promoting the reductive cleavage of the S–S bond in **V**. Each of these processes is energetically feasible (see ESI for full computational details†). Additionally, the quantum yield (Φ) value for the transformation was found to be 0.35, which suggests that a chain process is possibly not operating. Thus, the formate radical anion is unlikely to be contributing to the reduction of **2**.^{30,33,36,57}

From this point, the formed C-centered radical anion species **A**^{•-} undergoes a spin-center shift (SCS)⁵⁸ to form the

electrophilic *gem*-difluoromethyl radical intermediate **C**[•], which was also observed as a TEMPO adduct in the control experiments. DFT computations suggest that the SCS proceeds through a stepwise 1,2-F migration pathway (**TS-A-B**), wherein the fluorine on the terminal carbon shifts to the carbonyl carbon. This process is energetically feasible ($\Delta G^\ddagger = 13.3$ kcal mol⁻¹). Following the 1,2-F migration, the fluoride is released as an anion (*via* coordination with sodium from sodium formate) which forms the carbon-centered radical **C**[•].⁵⁹ In turn, alkyl radical **C**[•] then undergoes regioselective and irreversible Giese addition to the olefin moiety of the *N*-arylmethacrylamide (**1**) to form the radical intermediate **D**[•]. Finally, a facile radical cyclization followed by rearomatization would take place to furnish the difluorinated oxindole **3**. The DFT calculation indicated that this latter is likely to be proceeding *via* a HAT mechanism, where the hydrogen can be abstracted by the radical intermediate carbon centered radical **C**[•], which is being formed in excess in the reaction medium. Other radical intermediates, such as **A**^{•-} and $\text{CO}_2^{\cdot-}$, could be operative in this mechanism as well, however, the pathway *via* **C**[•] hydrogen abstraction is more energetically feasible. A second reaction mechanism for the rearomatization step would involve a single electron oxidation of **E**[•] by the thiyl radical **IV** to provide the corresponding carbocation intermediate, which after proton loss would furnish the final difluorinated compound **3**. Although this pathway (Fig. S11, ESI†) is slightly less energetically favorable than the radical HAT pathways described, the reaction is still energetically feasible and the rearomatization process is irreversible.

Conclusions

The photoinduced protocol developed herein represents a mechanistically distinct pathway to install fluorinated motifs easily onto *N*-arylmethacrylamides *via* a single, chemoselective C–F bond activation of trifluoroacetates, -acetamides, and



-arenes. The preparation of a library of valuable oxindole derivatives was accomplished under mild reaction conditions using the thiolate excited state as an organophotocatalyst. DFT computational results supporting the proposed reaction pathway complement the experimental studies and shed light on the reactivity of these readily available and powerful catalytic species. Taking advantage of the operational simplicity of the method, the reaction was performed under open-to-air conditions, allowing an easy scale-up for the multigram preparation of a target molecule. This protocol complements the synthetic tools available to install *gem*-difluoromethyl radicals *via* C–F activation, avoiding the use of rare metal-based catalysts and the use of expensive halogen-difluoroacetates as radical sources. Given the relevance and challenges found in this synthetic approach, the practical and accessible procedure described herein contributes to the advancement of the field of selective C–F bond activation and extends chemical space of important fluorinated motifs, unlocking new opportunities to explore the powerful reduction potential of excited thiolates in further transformations under photocatalytic conditions.

Data availability

The ESI† includes all experimental details, including quantum yield measurements, mechanistic studies, DFT calculation, synthesis and characterization of all products reported in this study. NMR spectra of all products are included as well.

Author contributions

All authors have given approval to the final version of the manuscript.

Conflicts of interest

There are no conflicts to declare.

Acknowledgements

The authors are grateful for the financial support (RG2020) provided by Merck KGaA, Darmstadt, Germany, and NIGMS (R35 GM 131680 to G. A. M.). The NSF Major Research Instrumentation Program (award NSF CHE-1827457), the NIH supplement awards 3R01GM118510-03S1 and 3R01GM087605-06S1, as well as the Vagelos Institute for Energy Science and Technology supported the purchase of the NMRs used in this study. O. G. gratefully acknowledges the NIGMS NIH (R35GM137797) and Camille and Henry Dreyfus Foundation for funding and Texas A&M University HPRC resources (<https://hprc.tamu.edu>), UMD Deepthought2, MARCC/BlueCrab HPC clusters and XSEDE (CHE160082 and CHE160053) for computational resources. The authors thank Dr Venkatesh Yarra (UPenn) for helping in the quenching experiments.

Notes and references

- 1 H. Amii and K. Uneyama, *Chem. Rev.*, 2009, **109**, 2119–2183.

- 2 A. Das and N. Chatani, *ACS Catal.*, 2021, **11**, 12915–12930.
- 3 S. Li and W. Shu, *Chem. Commun.*, 2022, **58**, 1066–1077.
- 4 D. O'Hagan, *Chem. Soc. Rev.*, 2008, **37**, 308–319.
- 5 K. Reichenbacher, H. I. Suss and J. Hulliger, *Chem. Soc. Rev.*, 2005, **34**, 22–30.
- 6 Z. H. Wang, Y. Sun, L. Y. Shen, W. C. Yang, F. Meng and P. H. Li, *Org. Chem. Front.*, 2022, **9**, 853–873.
- 7 P. J. Xia, Z. P. Ye, Y. Z. Hu, J. A. Xiao, K. Chen, H. Y. Xiang, X. Q. Chen and H. Yang, *Org. Lett.*, 2020, **22**, 1742–1747.
- 8 J. Wang, B. Huang, Y. Gao, C. Yang and W. Xia, *J. Org. Chem.*, 2019, **84**, 6895–6903.
- 9 X. Sun and T. Ritter, *Angew. Chem., Int. Ed.*, 2021, **60**, 10557–10562.
- 10 A. Singh, J. J. Kubik and J. D. Weaver, *Chem. Sci.*, 2015, **6**, 7206–7212.
- 11 A. Singh, C. J. Fennell and J. D. Weaver, *Chem. Sci.*, 2016, **7**, 6796–6802.
- 12 S. M. Senaweera, A. Singh and J. D. Weaver, *J. Am. Chem. Soc.*, 2014, **136**, 3002–3005.
- 13 S. Senaweera and J. D. Weaver, *J. Am. Chem. Soc.*, 2016, **138**, 2520–2523.
- 14 H. Wang and N. T. Jui, *J. Am. Chem. Soc.*, 2018, **140**, 163–166.
- 15 D. B. Vogt, C. P. Seath, H. Wang and N. T. Jui, *J. Am. Chem. Soc.*, 2019, **141**, 13203–13211.
- 16 J. B. I. Sap, N. J. W. Straathof, T. Knauber, C. F. Meyer, M. Medebielle, L. Buglioni, C. Genicot, A. A. Trabanco, T. Noel, C. W. Am Ende and V. Gouverneur, *J. Am. Chem. Soc.*, 2020, **142**, 9181–9187.
- 17 K. Chen, N. Berg, R. Gschwind and B. König, *J. Am. Chem. Soc.*, 2017, **139**, 18444–18447.
- 18 T. Xiao, L. Li and L. Zhou, *J. Org. Chem.*, 2016, **81**, 7908–7916.
- 19 S. B. Lang, R. J. Wiles, C. B. Kelly and G. A. Molander, *Angew. Chem., Int. Ed.*, 2017, **56**, 15073–15077.
- 20 L. Li, T. Xiao, H. Chen and L. Zhou, *Chem. - Eur. J.*, 2017, **23**, 2249–2254.
- 21 J. P. Phelan, S. B. Lang, J. Sim, S. Berritt, A. J. Peat, K. Billings, L. Fan and G. A. Molander, *J. Am. Chem. Soc.*, 2019, **141**, 3723–3732.
- 22 R. J. Wiles, J. P. Phelan and G. A. Molander, *Chem. Commun.*, 2019, **55**, 7599–7602.
- 23 Y. Q. Guo, R. Wang, H. Song, Y. Liu and Q. Wang, *Org. Lett.*, 2020, **22**, 709–713.
- 24 L. H. Wu, J. K. Cheng, L. Shen, Z. L. Shen and T. P. Loh, *Adv. Synth. Catal.*, 2018, **360**, 3894–3899.
- 25 H. Tian, Q. Xia, Q. Wang, J. Dong, Y. Liu and Q. Wang, *Org. Lett.*, 2019, **21**, 4585–4589.
- 26 J. L. Wang, B. B. Huang, C. Yang and W. J. Xia, *Chem. Commun.*, 2019, **55**, 11103–11106.
- 27 C. Zhu, Y. F. Zhang, Z. Y. Liu, L. Zhou, H. D. Liu and C. Feng, *Chem. Sci.*, 2019, **10**, 6721–6726.
- 28 S. L. Xie, X. T. Gao, H. H. Wu, F. Zhou and J. Zhou, *Org. Lett.*, 2020, **22**, 8424–8429.
- 29 Y. Li, X. Li, X. Li and D. Shi, *Chem. Commun.*, 2021, **57**, 2152–2155.
- 30 M. W. Campbell, V. C. Polites, S. Patel, J. E. Lipson, J. Majhi and G. A. Molander, *J. Am. Chem. Soc.*, 2021, **143**, 19648–19654.



- 31 C. Liu, K. Li and R. Shang, *ACS Catal.*, 2022, **12**, 4103–4109.
- 32 C. Liu, N. Shen and R. Shang, *Nat. Commun.*, 2022, **13**, 354.
- 33 J. H. Ye, P. Bellotti, C. Heusel and F. Glorius, *Angew. Chem., Int. Ed.*, 2022, **61**, e202115456.
- 34 S. Ghosh, Z. W. Qu, S. Pradhan, A. Ghosh, S. Grimme and I. Chatterjee, *Angew. Chem., Int. Ed.*, 2022, **61**, e202115272.
- 35 J. Lu, N. S. Khetrapal, J. A. Johnson, X. C. Zeng and J. Zhang, *J. Am. Chem. Soc.*, 2016, **138**, 15805–15808.
- 36 S. S. Yan, S. H. Liu, L. Chen, Z. Y. Bo, K. Jing, T. Y. Gao, B. Yu, Y. Lan, S. P. Luo and D. G. Yu, *Chem*, 2021, **7**, 3099–3113.
- 37 R. K. Dhungana, A. Granados, M. Sharique, J. Majhi and G. A. Molander, *Chem. Commun.*, 2022, **58**, 9556–9559.
- 38 A. Granados, R. K. Dhungana, M. Sharique, J. Majhi and G. A. Molander, *Org. Lett.*, 2022, **24**, 4750–4755.
- 39 G. Levitre, A. Granados, M. J. Cabrera-Afonso and G. A. Molander, *Org. Lett.*, 2022, **24**, 3194–3198.
- 40 G. Cerchiaro and A. M. D. Ferreira, *J. Braz. Chem. Soc.*, 2006, **17**, 1473–1485.
- 41 C. Marti and E. M. Carreira, *Eur. J. Org. Chem.*, 2003, 2209–2219.
- 42 C. V. Galliford and K. A. Scheidt, *Angew. Chem., Int. Ed.*, 2007, **46**, 8748–8758.
- 43 W. J. Fu, M. Zhu, G. L. Zou, C. Xu and Z. Q. Wang, *Asian J. Org. Chem.*, 2014, **3**, 1273–1276.
- 44 X. L. Wang, W. Wan, Y. R. Chen, J. L. Li, H. Z. Jiang, Y. Wang, H. M. Deng and J. Hao, *Eur. J. Org. Chem.*, 2016, 3773–3779.
- 45 D. Liu, S. B. Zhuang, X. Chen, L. Yu, Y. Q. Yu, L. Hu and Z. Tan, *Tetrahedron Lett.*, 2018, **59**, 612–616.
- 46 S. D. Ma, P. S. Zhou, X. Fan, D. J. Li and J. H. Yang, *Tetrahedron Lett.*, 2022, **102**, 153933.
- 47 H. Y. Li, X. X. Tang, J. H. Pang, X. Y. Wu, E. K. L. Yeow, J. Wu and S. Chiba, *J. Am. Chem. Soc.*, 2021, **143**, 481–487.
- 48 H. Li, Y. Liu and S. Chiba, *Chem. Commun.*, 2021, **57**, 6264–6267.
- 49 F. Kobayashi, M. Fujita, T. Ide, Y. Ito, K. Yamashita, H. Egami and Y. Hamashima, *ACS Catal.*, 2021, **11**, 82–87.
- 50 S. Wang, H. Wang and B. König, *J. Am. Chem. Soc.*, 2021, **143**, 15530–15537.
- 51 P. Xu, X. Y. Wang, Z. Wang, J. Zhao, X. D. Cao, X. C. Xiong, Y. C. Yuan, S. Zhu, D. Guo and X. Zhu, *Org. Lett.*, 2022, **24**, 4075–4080.
- 52 J. H. Ye, P. Bellotti, C. Heusel and F. Glorius, *Angew. Chem., Int. Ed.*, 2022, **61**, e202115456.
- 53 C. M. Q. Le, F. Morlet-Savary and A. Chemtob, *Polym. Chem.*, 2021, **12**, 6594–6605.
- 54 Z. S. Liu, S. Zhong, X. C. Ji, G. J. Deng and H. W. Huang, *ACS Catal.*, 2021, **11**, 4422–4429.
- 55 P. Saraswat, G. Jeyabalan, M. Z. Hassan, M. U. Rahman and N. K. Nyola, *Synth. Commun.*, 2016, **46**, 1643–1664.
- 56 B. T. Matsuo, P. H. R. Oliveira, E. F. Pissinati, K. B. Vega, I. S. de Jesus, J. T. M. Correia and M. Paixão, *Chem. Commun.*, 2022, **58**, 8322–8339.
- 57 C. M. Hendy, G. C. Smith, Z. H. Xu, T. Q. Lian and N. T. Jui, *J. Am. Chem. Soc.*, 2021, **143**, 8987–8992.
- 58 B. Matsuo, A. Granados, J. Majhi, M. Sharique, G. Levitre and G. A. Molander, *ACS Org. Inorg. Au*, 2022, **6**, 435–454.
- 59 Y. J. Yu, F. L. Zhang, T. Y. Peng, C. L. Wang, J. Cheng, C. Chen, K. N. Houk and Y. F. Wang, *Science*, 2021, **371**, 1232–1240.

